NEUROSCIENCE
RESEARCH ARTICLE
P. Qin et al. / Neuroscience 379 (2018) 142–151

Vascular-metabolic and GABAergic Inhibitory Correlates of Neural Variability Modulation. A Combined fMRI and PET Study

Pengmin Qin, [a,b,c,d,e†] **Niall W. Duncan,** [b,c,f*†] **David Yen-Ting Chen,** [c,g] **Chi-Jen Chen,** [g] **Li-Kai Huang,** [h] **Zirui Huang,** [i] **Chien-Yuan E. Lin,** [j] **Christine Wiebking,** [k] **Che-Ming Yang,** [l] **Georg Northoff** [b,c,h,m,n] **and Timothy J. Lane** [b,c,o*]

[a] *Guangdong Key Laboratory of Mental Health and Cognitive Science, South China Normal University, Guangzhou, China*

[b] *Graduate Institute of Humanities in Medicine, Taipei Medical University, Taipei, Taiwan*

[c] *Brain and Consciousness Research Centre, Taipei Medical University-Shuang Ho Hospital, New Taipei City, Taiwan*

[d] *Centre for Studies of Psychological Applications, South China Normal University, Guangzhou, China*

[e] *School of Psychology, South China Normal University, Guangzhou, China*

[f] *Centre for Cognition and Brain Disorders, Hangzhou Normal University, Hangzhou, China*

[g] *Department of Radiology, Taipei Medical University-Shuang Ho Hospital, New Taipei City, Taiwan*

[h] *Department of Neurology, Taipei Medical University-Shuang Ho Hospital, New Taipei City, Taiwan*

[i] *Mind, Brain Imaging and Neuroethics Research Unit, Institute of Mental Health Research, University of Ottawa, Ottawa, Canada*

[j] *GE Healthcare, Taipei, Taiwan*

[k] *Applied Emotion and Motivation Research, Institute for Psychology and Education, Universität Ulm, Ulm, Germany*

[l] *Department of Nuclear Medicine, Shuang Ho Hospital, Taipei Medical University, New Taipei City, Taiwan*

[m] *University of Ottawa Brain and Mind Research Institute, Centre for Neural Dynamics, Faculty of Medicine, University of Ottawa, Ottawa, Canada*

[n] *Mental Health Centre, Zhejiang University School of Medicine, Hangzhou, Zhejiang Province, China*

[o] *Research Center for Mind, Brain, and Learning, National Chengchi University, Taipei, Taiwan*

Abstract—Neural activity varies continually from moment to moment. Such temporal variability (TV) has been highlighted as a functionally specific brain property playing a fundamental role in cognition. We sought to investigate the mechanisms involved in TV changes between two basic behavioral states, namely having the eyes open (EO) or eyes closed (EC) *in vivo* in humans. To these ends we acquired BOLD fMRI, ASL, and [^{18}F]-fluoro-deoxyglucose PET in a group of healthy participants (n = 15), along with BOLD fMRI and [^{18}F]-flumazenil PET in a separate group (n = 19). Focusing on an EO- vs EC-sensitive region in the occipital cortex (identified in an independent sample), we show that TV is constrained in the EO condition compared to EC. This reduction is correlated with an increase in energy consumption and with regional $GABA_A$ receptor density. This suggests that the modulation of TV by behavioral state involves an increase in overall neural activity that is related to an increased effect from GABAergic inhibition in addition to any excitatory changes. These findings contribute to our understanding of the mechanisms underlying activity variability in the human brain and its control.

Key words: temporal variability, brain state, cerebral blood flow, visual cortex, GABAA receptor, flumazenil.

INTRODUCTION

Neural activity varies continually from moment to moment. Such neuronal temporal variability (TV) is the target of increasing amounts of research and has been measured through a number of techniques, including blood-oxygen-level-dependent (BOLD) fMRI (Garrett et al., 2013). Recent work has shown that TV in different brain regions can be been linked to individual differences in, for example, visual discrimination thresholds (Wutte et al., 2011), task accuracy (Armbruster-Genc et al., 2016; Mennes et al., 2011), and peripersonal space

*Corresponding authors. Address: Brain and Consciousness Research Centre, Taipei Medical University, 172 Keelung Road, Section 2, Taipei, Taiwan (N. W. Duncan). Graduate Institute of Humanities in Medicine, Taipei Medical University, 250 Wuxing Street, Taipei, Taiwan (T. J. Lane).
E-mail addresses: niall.w.duncan@gmail.com (N. W. Duncan), timlane@tmu.edu.tw (T. J. Lane).
† These authors contributed equally to the work.
Abbreviations: ASL, arterial spin labeling; BOLD, blood-oxygen-level-dependent; CSF, cerebrospinal fluid; EC, eyes closed; EO, eyes open; FDG-PET, [^{18}F]-fluoro-deoxyglucose PET; FMZ-PET, [^{18}F]-flumazenil PET; GM, gray matter; PET, positron-emission-tomography; rCBF, regional cerebral blood flow; TV, temporal variability; WM, white matter.

https://doi.org/10.1016/j.neuroscience.2018.02.041
0306-4522/

(Ferri et al., 2015). As well as this, TV has been reported to be altered in a number of psychiatric and neurological disorders, including Alzheimer's disease (Takahashi, 2013) and bipolar disorder (Martino et al., 2016). Importantly, TV is not a fixed property of the brain but is instead modulated by different tasks and stimuli (Garrett et al., 2012, 2014). Taken together, this evidence suggests that TV is a functionally specific brain property that plays a fundamental role in cognition. Despite this apparent importance, the mechanisms underlying TV and its change between specific behavioral contexts remain to be fully explored *in vivo* in humans.

Previous work has shown that neural TV, as measured with BOLD fMRI, correlates well with the amount of energy consumed locally, as measured through glucose consumption (Aiello et al., 2015; Nugent et al., 2015). This link presents an opportunity for gaining insight into what mechanisms are related to the modulation of TV according to behavioral state. For example, it has been observed that switching from an eyes closed (EC) to eyes open (EO) condition results in a reduction in TV (Bianciardi et al., 2009; Jao et al., 2012; Zou et al., 2015). Given this, the first aim of this study was to use these EC to EO changes to investigate the energetic processes supporting the neural changes reflected in TV modulation, asking whether changes in TV lead to concurrent changes in local energy usage. BOLD fMRI was used to quantify TV while [^{18}F]-fluorodeoxyglucose PET (FDG-PET) was used as a measure of regional glucose, and as such energy, consumption (rMRGlu). Regional cerebral blood flow (rCBF), as measured with arterial spin labeling (ASL), was used as an additional proxy measure of energy consumption due to the known coupling between rCBF and glucose uptake during both rest and task states (Cha et al., 2013; Galazzo et al., 2016; Newberg et al., 2005). This additional measure was used to circumvent issues relating to scanning participants in two different states with PET. The three types of data were acquired in the same participants (Dataset 1 – see Fig. 1).

Since opening the eyes is primarily a visual stimulus, the study focussed on the occipital cortex. The relevant brain areas were identified in an independent sample using an EO/EC block-design experiment and applied to the main datasets. A region-based analysis of the EO/EC fMRI and ASL data, along with EC FDG-PET, was then conducted (He, 2011; Huang et al., 2016; Nugent et al., 2015). The validity of rCBF as a measure of energy consumption in this region was confirmed by correlating EC rMRGlu with the EC ASL data (Cha et al., 2013). It was hypothesized that TV would be reduced in the EO condition, as compared to EC (Bianciardi et al., 2009; Jao et al., 2012). At the same time, based on previous work using FDG-PET, rCBF (and thus energy consumption) was expected to increase with the opening of the eyes (Riedl et al., 2014). We thus hypothesized that changes in TV between EC and EO would be negatively correlated with rCBF changes.

The modulation in the visual cortex of the variability of excitatory responses over time by inhibitory interneurons has been studied previously in non-human animals

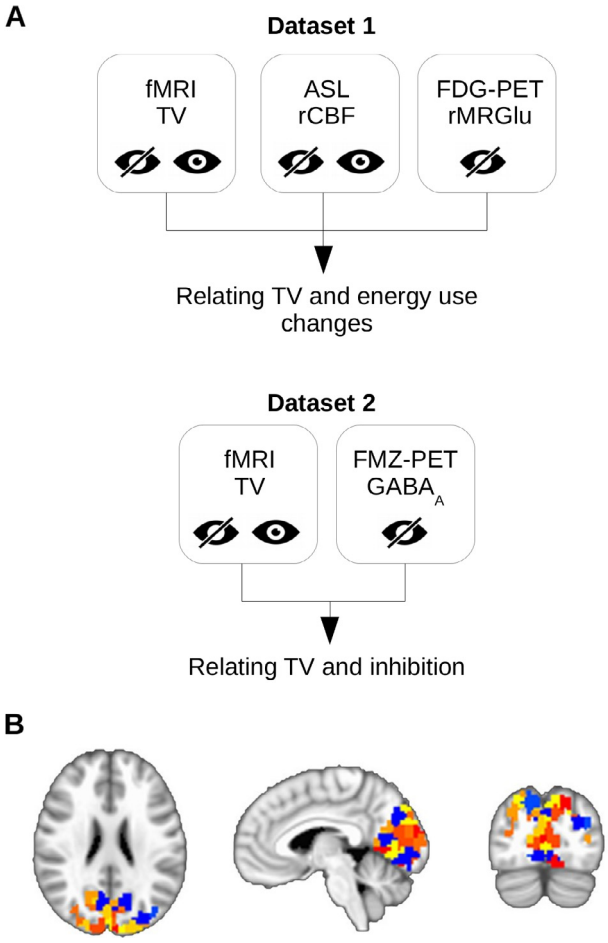

Fig. 1. (A) Two separate datasets were used in the analysis. Dataset 1 (upper section) consisted of BOLD fMRI for measuring temporal variability, ASL for measuring regional cerebral blood flow (rCBF), and FDG-PET for measuring glucose consumption. Dataset 2 (lower section) consisted of BOLD fMRI and FMZ-PET for measuring GABAA receptor density. (B) Mean values for each data type were extracted from a set of 99 ROIs located in the occipital cortex (note that four ROIs were then excluded due to high TV values).

(Fingelkurts et al., 2004; Sabolek et al., 2012; Shew et al., 2011; Xiao et al., 2012). This role for inhibition in structuring activity over time has not been studied in humans, however. Notably, though, evidence from work linking instantaneous responses, such as BOLD effect amplitudes, to GABAergic activity provides background evidence for the relationship between inhibition and neuroimaging measures in humans (Duncan et al., 2014). Accordingly, the second aim of the study was to relate TV in the occipital cortex to GABAergic activity. To do so we utilized [^{18}F]-flumazenil PET (FMZ-PET) data as a measure of $GABA_A$ receptors (Prevett et al., 1995), along with BOLD fMRI data from the same participants to quantify TV (Dataset 2 – see Fig. 1). The same region-based approach was taken as with Dataset 1. The change in TV between EC and EO was calculated and then correlated with regional $GABA_A$ receptor density. It was assumed that regions with more $GABA_A$ receptors have a greater potential for inhibitory action (see *Discussion*, below, for more on this point) and so it

was hypothesized that these regions would display a greater reduction in TV with the opening of the eyes.

EXPERIMENTAL PROCEDURES

Dataset 1 – fMRI, ASL, and FDG-PET

Participants. Seventeen healthy volunteers participated in this part of the study (9 female; mean age = 31.9 years; age range = 23–58 years). Two participants had unusable ASL data and so all data from these participants (ASL, BOLD, and FDG-PET) were excluded from the analysis (15 remaining participants, 8 female; mean age = 30.7 years; age rage = 25–58 years). None of the participants had a history of neurological or psychiatric disorders, nor were taking medication at the time of scanning. Standard MRI exclusion criteria were employed. All participants gave their written informed consent and were compensated financially for their time. The study was approved by the Taipei Medical University Institutional Review Board.

Both the PET and MRI scanning were done at the Taipei Medical University Shuang Ho Hospital. All scans were conducted in the morning, with the PET scan completed first, followed by the MRI. The time of each scan was the same for all participants, reducing time-of-day effects on the data (Duncan and Northoff, 2012).

MRI data acquisition. MR images were acquired on a GE MR750 3 Tesla scanner using a standard 8-channel head coil. A high-resolution T1-weighted anatomical image was acquired first. Following this, the BOLD and ASL imaging was carried out, with the order of these scans counterbalanced across participants. EO and EC runs were carried out for both BOLD and ASL. The EO/EC orders for BOLD and rCBF were also counterbalanced across participants. The lights in the scanner room were turned off during scanning. During both types of scans, participants were instructed to lie still, to stay awake, and to not focus their attention on anything in particular. In EC runs the participants kept their eyes closed throughout and a black screen was presented to ensure that they were exposed to little light. During EO runs a gray screen was presented. In these runs participants were instructed to keep their eyes open and to look toward the screen. Participants were asked after scanning if they had remained awake; none reported falling asleep.

BOLD-sensitive images were acquired using a $T2^*$-weighted EPI sequence (TR = 2000 ms; TE = 30 ms; flip angle = 90°; FoV = 220 mm; matrix = 64 × 64; slice thickness = 3.4 mm; slice gap = 0 mm; 33 slices). 200 volumes were acquired in each run (6.67 min). rCBF images were acquired using a 3D pCASL ASL sequence with a fast spin echo acquisition for vessel suppression (TR = 5327 ms; TE = 10.5 ms; FoV = 220 mm; slice thickness = 4 mm; slice gap = 0 mm; 38 slices; NEX = 4; labeling duration = 1500 ms; post-labeling delay = 1525 ms). Each ASL scan lasted for 6.63 min.

FDG-PET data acquisition and pre-processing. PET data were acquired on a GE Discovery ST PET-CT scanner. Participants were asked to fast for eight hours prior to the scan session. [^{18}F]-fluorodeoxyglucose (mean dose = 11.8 mCi ± 1.2 SD) was administered intravenously, following which participants rested in a darkened room with their eyes closed for 40 min. They were instructed to remain awake during this time. A 20-min scan was then conducted with the eyes closed. Note that FDG-PET was not used to measure energy use in both EO and EC due to ethical and practical barriers to administering two radiation doses to participants in a short space of time.

Image reconstruction was done using an iterative process implemented in the manufacturer provided software. The reconstructed images were then aligned to the MNI standard space in the same manner as the BOLD and ASL images, resampled to 3-mm isotropic voxels, and smoothed with a 6-mm kernel. Global differences between participants in the estimates of rMRGlu were removed by dividing each voxel's value by the whole-brain mean.

Dataset 2 – fMRI and FMZ-PET

Participants. Twenty-seven participants took part in the study (10 female; mean age = 22.3 years; age range = 18–34 years). Two of these did not attend the PET scanning session and six had too much head motion during the fMRI scan (> 2 mm), leaving 19 participants with usable fMRI and FMZ-PET data (8 female; mean age = 23.1 years; age range = 18–34 years). None of the participants had a history of neurological or psychiatric disorders, nor were taking medication at the time of scanning. Standard MRI exclusion criteria were employed. All participants gave their written informed consent and were compensated financially for their time. The study was approved by the McGill University ethics committee. An independent analysis of this dataset has been published elsewhere (Qin et al., 2012). Both the PET and MRI scanning were done at the Montreal Neurological Institute. MRI and FMZ-PET data were acquired on different days in a randomized order (mean time between scans = 1.9 ± 3.6 days).

MRI data acquisition. MR images were acquired on a Siemens Trio 3 Tesla scanner using a 32-channel head coil. BOLD-sensitive images were acquired using a $T2^*$-weighted EPI sequence (TR = 2270 ms; TE = 25 ms; flip angle = 90°; FoV = 205 mm; matrix = 64 × 64; slice thickness = 3.2 mm; slice gap = 0 mm; 47 slices). 467 volumes were acquired in each run (17.7 min). A high-resolution T1-weighted anatomical image was also acquired.

The functional run was split into two parts. The first part was an EO/EC block design experiment that was not analyzed here. The second part consisted of four long EO and EC periods of equal length (total length = 215 volumes, 8.1 min) that alternated (2 × EO, 2 × EC; order counterbalanced across participants). Tones were

used to indicate when participants should open or close their eyes. A camera was used to ensure that participants were correctly following these cues. During the scan period participants were instructed to relax and to remain awake. For the TV analysis the two EO and the two EC periods were concatenated into single data blocks.

FMZ-PET data acquisition and pre-processing. Positron-emission-tomography (PET) imaging with [^{18}F]-flumazenil, a benzodiazepine antagonist that binds at the $GABA_A$ benzodiazepine site. This method has been widely used to measure $GABA_A$ receptor density *in vivo* in humans (Frey et al., 1991; Salmi et al., 2008). Whole-brain [^{18}F]-flumazenil binding potential (BP_{ND}) values was obtained using a Siemens ECAT High Resolution Research Tomograph PET system. A 6-min transmission scan (^{137}Cs-point source) was first acquired for attenuation correction followed by an intravenous tracer injection (over 60 s) of 260.7 MBq (±21.24 SD) of [^{18}F]FMZ. Subjects were instructed to close their eyes and remain awake for 60 min during data acquisition.

List-mode data were acquired for a period of 60 min and then binned into a series of 26 sequential sets. PET data were reconstructed using a 3D OP-OSEM algorithm (10 iterations and 16 subsets) (Hudson and Larkin, 1994; Hong et al., 2007), with full accounting for scatter, random coincidences, attenuation, decay, dead-time, and frame-based motion correction (Costes et al., 2009). Voxel-wise $GABA_A$ receptor binding potential maps were then calculated with the Logan plot method (Logan et al., 1996) using the pons as the reference region. The resulting images had a voxel size of 1.22 × 1.22 × 1.22 mm3 (256 × 256 × 207 voxels).

MRI data pre-processing for Dataset 1 and Dataset 2

All MRI data were processed using the AFNI (https://afni.nimh.nih.gov/afni/), ANTs (http://stnava.github.io/ANTs/), and FSL (http://fsl.fmrib.ox.ac.uk/fsl/fslwiki/) software packages. In a first step, the anatomical images were skull-stripped and then segmented into gray matter (GM), white matter (WM), and cerebrospinal fluid (CSF) compartments. The anatomical images were then normalized to the MNI standard space through a series of rigid body, affine, and SyN alignments (ANTs). WM and CSF masks were created by thresholding the relevant tissue maps at 1 (from a range of 0 to 1), binarizing them, and then eroding them by two voxels.

For the BOLD datasets, the first five volumes were discarded to avoid saturation effects. The data were then slice-time corrected; corrected for head motion; masked to remove the skull; and detrended. Alignments between the BOLD and anatomical images were then calculated. Mean timeseries from the WM and CSF were extracted using the previously created masks (these were transformed into the native space of the BOLD images) and the first three principal components from each timecourse calculated (Behzadi et al., 2007). These were regressed out of the data along with the six head motion parameters obtained during head motion correction, their temporal derivatives, and first- and second-degree polynomial trends. Finally, the data were aligned to the MNI template (via the anatomical images), were resampled to 3-mm isotropic voxels, and were smoothed using a 6 mm at full-width half-maximum Gaussian kernel.

Global differences in rCBF between participants were removed from the ASL data by dividing each voxel by the mean value across the whole brain (Chen et al., 2011). The brain mask was obtained from the BET skull-stripping tool. Following this, the ASL images were aligned with the MNI standard space template (via the anatomical images), resampled to 3-mm isotropic voxels, and smoothed with a 6-mm kernel.

ROI creation

A third, independent, fMRI dataset was used to define the occipital regions sensitive to the opening and closing of the eyes. In this, 19 healthy volunteers (5 female; mean age = 28.2 years (±9.06 SD); age range = 23–55 years) undertook a block-design task in which they opened and closed their eyes. EO blocks were contrasted with EC in a standard GLM analysis. The brain area of interest was identified by thresholding the resulting statistical maps at $p < 0.001$ (uncorrected). This produced a region encompassing the occipital cortex with a total volume of 83160 mm^3 (3080 voxels) which was then split into 99 randomly seeded ROIs (Fig. 1B), each with a volume of approximately 840 mm^3 (31 voxels).

Data extraction for Dataset 1 and Dataset 2

The visual cortex ROIs were firstly applied to the BOLD data and the mean timeseries for each calculated. These timeseries were then converted to percent signal change values and band-pass filtered between 0.01 and 0.08 Hz to minimize the contribution of physiological noise. The TV of these filtered timeseries was calculated as the mean squared successive difference of the signal (Samanez-Larkin et al., 2010). This reflects how much the signal changes from one datapoint to the next and has been taken to represent the temporal specificity of neural activation within a region. TV values were then averaged in each ROI across participants for each fMRI dataset, giving values per region for the EO and EC runs.

The same ROIs were then applied to the ASL data to obtain group-mean rCBF values for each region in the EO and EC conditions. An additional partial volume correction step was applied to each participant's data prior to averaging. The following equation was applied to the rCBF values for each ROI: corrected rCBF = original rCBF/(GM proportion + 0.4*WM proportion) (Chen et al., 2011). WM and GM proportions were calculated from the previously calculated tissue segmentations. The 0.4 factor represents the global ratio between WM and GM (Du et al., 2006). Four ROIs were found to have extreme TV values in either the EO or EC condition (>2.5 SD above the mean) and were thus excluded, leaving complete datasets from 95 ROIs. A similar procedure, including the partial volume correction, as was used for the rCBF values was then applied to the FDG-PET data.

The FMZ-PET data were also normalized and mean values from the ROIs extracted. Mean GM density values for each ROI were also calculated. At the end of these processing steps there were group-mean values for each of the 95 ROIs for the FDG-PET data (EC), BOLD fMRI data (EO/EC), and ASL data (EO/EC) for Dataset 1 and for the FMZ-PET (EC) and BOLD fMRI data (EO/EC) for Dataset 2.

Statistical analysis

The first question investigated was how well rCBF values corresponded to the glucose metabolism values obtained using FDG-PET (Dataset 1). This was done to confirm that the relationship between these two metrics described in other work was present in our own data (Chen et al., 2011; Galazzo et al., 2016). This was done by correlating the FDG-PET value with the EC rCBF (Spearman's). The relationship between glucose metabolism and TV was then investigated by correlating the rMRGlu values with EC TV. Finally, TV(EC) values were correlated with the rCBF(EC).

The next step in the analysis was then to identify how TV and rCBF are altered between EO and EC (Dataset 1). Mean values across all ROIs for each were firstly compared using paired sample *t*-tests. Changes in between EO and EC were also tested in the fMRI data from Dataset 2. Having described the changes in TV and rCBF between the two conditions, we then investigated how the changes in each of these metrics are related to each other. Differences in TV and rCBF between the states were calculated (EO-EC) and correlated with each other. Finally, the involvement of the GABAergic system in the modulation of TV by brain state was tested by correlating the change in TV between EO and EC with regional $GABA_A$ BP_{ND} values (Dataset 2). As it has been suggested that $GABA_A$ BP_{ND} values may represent neuronal integrity rather than $GABA_A$ receptors per se (la Fougère et al., 2011), we also correlated the EO-EC TV difference with FMZ while including GM density values as a control variable. In a final exploratory step we conducted a cross-dataset correlation between EO-EC rCBF and $GABA_A$ BP_{ND} values. This takes advantage of the use of group regional values which theoretically aim to represent the general population and as such can be compared.

All statistical analyses were carried out in Python using the Scipy (https://www.scipy.org) and Statsmodels (http://statsmodels.sourceforge.net/) toolboxes. Test or effect size statistic (Spearman's rho, Cohen's *d*) confidence intervals were calculated through bootstrapping (10,000 permutations). As a number of statistical comparisons were made in the analysis, type I errors were controlled through FDR correction.

Control analyses

The variability of the global signal, which alters between EO and EC (Wong et al., 2016), may influence TV results (Zou et al., 2015). As such, we carried out a number of control analyses to help rule out spurious results driven by any such effect. We selected the sensorimotor network from a previously published atlas (Yeo and Krienen, 2011) and segmented it into ROIs in the same manner as the visual region. The correlation between TV and rCBF values was calculated, followed by the correlation between the TV and rCBF EO-EC differences.

RESULTS

Relationship between TV, rCBF, and FDG-PET

Having calculated the group average values in each ROI for the target data (TV EO/EC, rCBF EO/EC, and eyes closed rMRGlu), the relationship between each datatype in the EC condition was investigated. It was found, firstly, that rCBF in the EC condition was strongly correlated with glucose metabolism, as measured with FDG-PET ($\rho = 0.81$ [95% CI = 0.71 0.88], $p_{FDR} < 0.01$; Fig. 2A). This suggests that rCBF can be used as a valid proxy for energy use in the specific regions studied. A positive correlation was then observed between glucose metabolism and EC BOLD TV ($\rho = 0.47$ [0.28 0.62], $p_{FDR} < 0.01$; Fig. 2B). This is supported by the fact that rCBF and TV were also found to be positively correlated during the EC condition ($\rho = 0.4$ [0.18 0.58], $p_{FDR} < 0.01$; Fig. 2C). A correlation

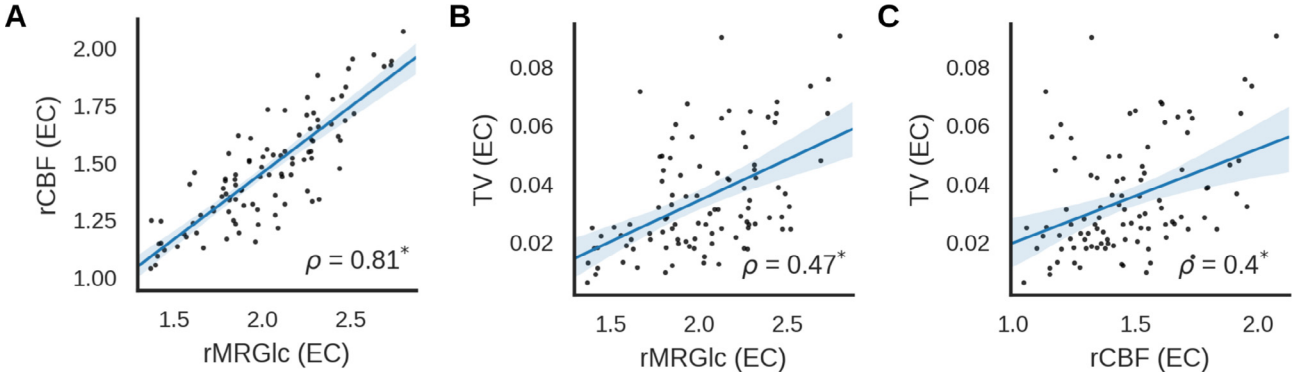

Fig. 2. (A) In Dataset 1, regional blood flow correlated strongly with glucose consumption during the eyes closed condition. Temporal variability during the eyes closed condition was positively correlated with both (B) glucose consumption and (C) blood flow. Each point in the plot indicates a single ROI. Lines show the best linear fit with the 95% confidence interval of this fit shown by the shaded area. rCBF = cerebral blood flow; EC = eyes closed; rMRGlu = glucose consumption; TV = temporal variability. * denotes $p_{FDR} < 0.01$.

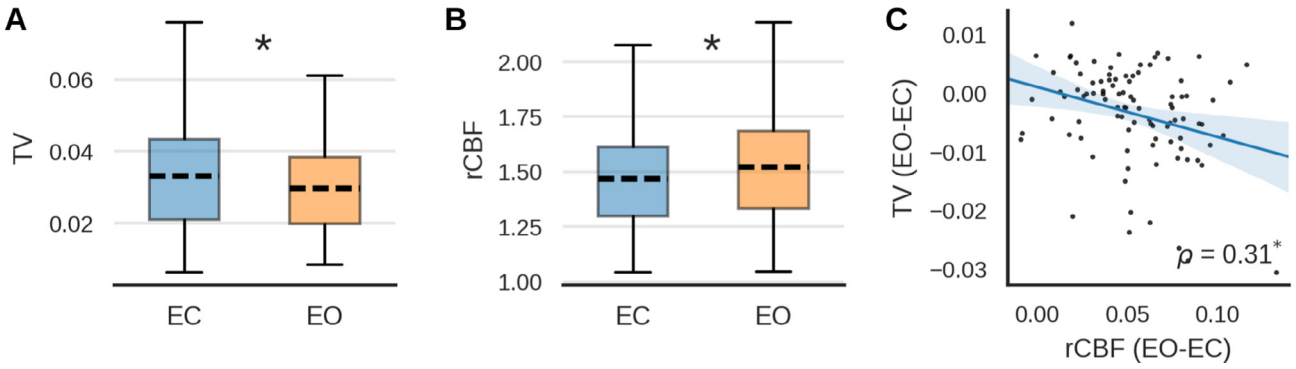

Fig. 3. (A) In Dataset 1, temporal variability was higher during eyes closed than during eyes open. (B) The opposite effect was seen for blood flow, which was higher during eyes open. Boxes indicate the quartile range, with the mean indicated by a horizontal line. (C) The eyes open vs eyes closed difference in temporal variability was negatively correlated with the difference in blood flow. Each point in the plot indicates a single ROI. Lines show the best linear fit with the 95% confidence interval of this fit shown by the shaded area. BP_{ND} = binding potential; rCBF = cerebral blood flow; EC = eyes closed; EO = eyes open; TV = temporal variability. * denotes $p_{FDR} < 0.01$.

between rCBF and TV was also seen in the EO condition ($\rho = 0.48$ [0.28 0.65], $p < 0.01$).

Change in TV and rCBF between EC and EO

Average TV and rCBF values were then compared between the EC and EO conditions (Dataset 1). Activity variability was found to be reduced in EO compared to EC ($t = 4.09$, $p_{FDR} < 0.01$, Cohen's $d = 0.21$ [0.12 0.27]; Fig. 3A). In contrast, mean rCBF increased in the EO condition, as compared to EC ($t = 18.2$, $p_{FDR} < 0.01$, Cohen's $d = 0.21$ [0.17 0.25]; Fig. 3B). The same change in TV was also observed in Dataset 2 ($t = 3.2$, $p < 0.01$, Cohen's $d = 0.12$ [0.05 0.19]) and with TV values normalized by the global mean ($t = 2.79$, $p < 0.01$, Cohen's $d = 0.15$ [0.09 0.48]). A decrease in TV in the visual cortex ROIs with the opening of the eyes thus corresponds with an increase in rCBF in the same regions.

Energy use in TV change

To investigate the relationship between TV and rCBF changes, the difference in TV and rCBF in each ROI between EC and EO were correlated. A negative correlation between the changes in each measure was observed ($\rho = -0.31$ [−0.11 −0.51], $p_{FDR} < 0.01$; Fig. 3C). The same effect was also seen when using TV values normalized by the SD of the global mean ($\rho = -0.29$ [−0.09 −0.48], $p < 0.01$). For the control analysis using the sensorimotor network, there was a positive correlation between EC TV and rCBF ($\rho = 0.34$ [0.10 0.54], $p_{FDR} < 0.01$) but no correlation between the EO-EC differences in each ($\rho = -0.12$, [−0.36 0.14], $p = 0.29$).

$GABA_A$ receptor involvement in TV change

Finally, the involvement of the GABAergic system in the modulation of TV between EO and EC was tested by correlating the TV change with local $GABA_A$ receptor density (Dataset 2). A negative correlation was observed ($\rho = -0.3$ [−0.12 −0.47], $p_{FDR} < 0.01$; Fig. 4A), suggesting that regions with a larger $GABA_A$ receptor population effect a greater change in TV between the two conditions. This correlation was also present when including regional gray matter density as a covariate, providing some support for the specificity of the effect to $GABA_A$ BP_{ND} ($\rho = -0.29$ [−0.1 −0.44], $p < 0.01$). It may also be noted that there was a positive correlation between TV and $GABA_A$ BP_{ND} during EC ($\rho = 0.25$ [0.05 0.44], $p = 0.01$) but not during EO ($\rho = 0.18$ [−0.04 0.38], $p = 0.08$). In addition, across the two datasets, $GABA_A$ receptor density was positively correlated with the difference in rCBF between EO and EC ($\rho = 0.39$ [0.18 0.54], $p_{FDR} < 0.01$; Fig. 4B).

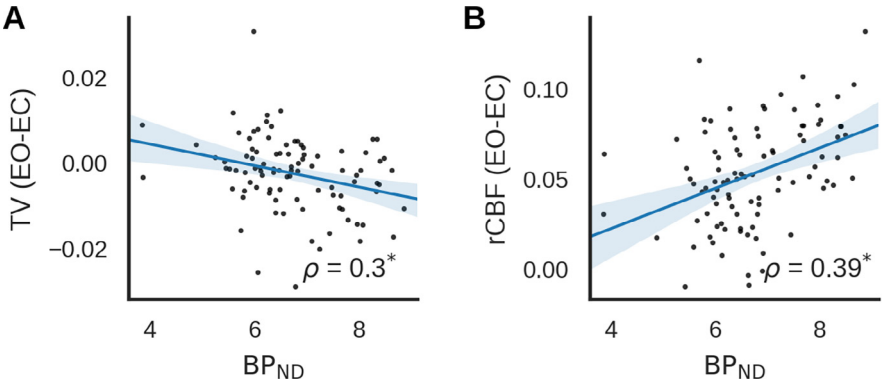

Fig. 4. (A) In Dataset 2, a negative correlation was seen between the EO vs EC change in temporal variability and regional $GABA_A$ receptor density. (B) The difference in rCBF between EO and EC (Dataset 1) was positively correlated with BP_{ND} (Dataset 2). Each point in the plot indicates a single ROI. Lines show the best linear fit with the 95% confidence interval of this fit shown by the shaded area. BP_{ND} = binding potential; rCBF = cerebral blood flow; EC = eyes closed; EO = eyes open; TV = temporal variability. * denotes $p_{FDR} < 0.01$.

DISCUSSION

In this study we sought to investigate the mechanisms involved in the modulation of BOLD signal variability over time in the human brain. This was done by relating changes in TV between two basic behavioral states – EO and EC – to measures of energy consumption (ASL and FDG-PET) and $GABA_A$ receptor density (FMZ-PET) in two independent datasets.

In a first step we showed that TV is positively correlated with glucose metabolism (Fig. 2B). During EC, regions that have greater activity variability over time were seen to have higher rMRGlu values. A similar positive correlation between TV and rMRGlu has been reported previously when taking the cortex as a whole (Aiello et al., 2015; Nugent et al., 2015). Such whole-brain analyses, however, leave open questions as whether or not the relationship remains when looking at particular sub-divisions of the brain (Liang et al., 2013). The current results show that, at least for the visual regions, a positive relationship between TV and rMRGlu can be confirmed. As rMRGlu is closely tied to neural signaling (Hyder and Rothman, 2011; Howarth, 2014; Hyder et al., 2013), this finding gives support to the assumption that BOLD TV represents fluctuations in neural function, rather than in other unrelated physiological or scanner-related properties (Logothetis, 2008; Ogawa et al., 1990).

Local glucose consumption has been shown to have a good general correlation with ASL measures of rCBF (Chen et al., 2011; Galazzo et al., 2016). There are, however, regional variations in how close this link is (Cha et al., 2013) and so we confirmed the correlation between FDG-PET and rCBF in the occipital cortex (in the EC condition) in order to validate the use of rCBF as a proxy for energy consumption. A strong positive correlation was observed ($\rho = 0.81$; Fig. 2A), demonstrating that regional glucose metabolism in the occipital cortex is closely linked to relative cerebral blood flow in the area (Jueptner and Weiller, 1995).

Having established this connection in the current data, the correlation between TV and rCBF during the EC condition was investigated. Based on the rMRGlu result, one would expect a positive correlation, which was indeed found (Fig. 2C). This is consistent with prior work involving rCBF and neural activity measures similar to TV (Li et al., 2012). Interestingly, the correlation coefficients for both rCBF and rMRGlu were comparable (0.4 and 0.47), lending weight to the assumption that both metrics are representing the same physiological processes when being correlated with TV. Additional support can also be found in prior work showing that there is a correlation between task-induced rCBF and rMRGlu changes in the visual cortex (Newberg et al., 2005). This is an important point for the analysis steps where rCBF during EO is used as a proxy for rMRGlu.

Comparing EO and EC, it was shown that TV in the visual cortex is higher in the latter than in the former (Fig. 3A). Again, this finding is consistent with previous studies (Bianciardi et al., 2009; Jao et al., 2012). In contrast, rCBF was found to be higher during EO than in EC (Fig. 3B). This increase in rCBF with the opening of the eyes is consistent with a prior ASL study (Hermes et al., 2007), and, given the link between rCBF and rMRGlu, with a prior FDG-PET study (Riedl et al., 2014). The reduction in variability may represent the visual cortex switching from a maximally dynamic state in the EC condition to a state that is constrained by external input in the EO condition (Deco et al., 2009; Deco and Jirsa, 2012). In other words, the ‘‘degrees of freedom” of neural activity within a region as a whole may be reduced by the introduction of an external stimulus (Garrett et al., 2014). It may be noted, however, that the reduction in TV is on average across the occipital region and that there are some ROIs that show an increase. Plotting the regions reveals that the decrease in TV occurs in lower visual regions while higher ones show no change or an increase. One may speculate that this distinction along the processing stream may reflect the impoverished visual input during the EO condition and that it may be modulated by more complex input.

The change in TV between EO and EC was negatively correlated with the change in rCBF (Fig. 3C). That a reduction in variability is correlated with an increase in rCBF (and, by extension, energy consumption) suggests that the reduction in TV requires energy. Combined with the positive correlation between TV and rCBF/rMRGlu during EC, these results suggest that the relationship between TV and energy consumption is more complex than a direct linear relationship. Notably, the visual stimulus induced changes in TV and rCBF were correlated with each other in the visual cortex but the control analysis showed no such effect in the sensorimotor network. This gives support to the effects discussed being related to neuronal activity rather than non-neuronal physiological effects.

The negative correlation between TV change (EO-EC) and $GABA_A$ receptor binding potential seen here provides support for inhibitory processes contributing to the modulation of TV in humans and further specifies the mechanism to one that involves this particular receptor subtype (although others may also be involved). This is consistent with work in non-human animals highlighting the role of $GABA_A$ receptors in influencing visual sensitivity through modulation of excitatory neural responses (Jirmann et al., 2009; Katzner et al., 2011). More generally, this GABAergic effect interacting with excitation to determine TV concurs with the view that balanced inhibition and excitation produces a stable activity regime (van Vreeswijk and Sompolinsky, 1996; Deco and Jirsa, 2012; Shew et al., 2011). Finally, we can note that the firing of inhibitory interneurons is an energy intensive process (Kann et al., 2014) for which glucose is the most effective metabolic substrate (Galow et al., 2014). Given this, any increase in inhibitory activity can be assumed to lead to an increase in glucose consumption. This will be in addition to the increase in excitatory energy demands brought about by the opening of the eyes (Barry et al., 2007). The positive correlation between rCBF changes and regional $GABA_A$ receptor binding reported here is in line with this supposition and links together the metabolic and neurotransmission related aspects of the findings.

A number of other considerations about the present study should also be mentioned. Firstly, for technical

and ethical reasons, FDG-PET was not administered during both EC and EO. Accordingly, the measures of energy use applied during the EO state are indirect via rCBF. The tight correlation between rCBF and rMRGlu in EC, in conjunction with prior research (Chen et al., 2011; Galazzo et al., 2016), suggests that this issue is unlikely to undermine our results. It would, however, be desirable to confirm them in a group where both EO and EC FDG-PET are available. Secondly, the different data-types were acquired on different occasions and on different scanners. Although the time of day at which the different scans occurred was kept the same, reducing the potential for an impact from this factor on the results, replicating the study using simultaneous PET-fMRI would be advantageous. Thirdly, there are some considerations regarding the interpretation of the BP_{ND} values. The numbers and binding properties of GABA receptors in a region are modified by endogenous release (Arancibia-Cárcamo and Kittler, 2009; Jacobson-Pick and Richter-Levin, 2012; Jacob et al., 2008; Jaffer et al., 2012; Liefaard et al., 2009). This means that high BP_{ND} values for an individual may represent an area with relatively lower endogenous release. The inter-region differences in group values used here are unlikely to reflect this feature, however, as the relative differences should average out. This supposition is supported by the similarity between the $GABA_A$ receptor maps obtained with PET and post-mortem receptor density counts (Eickhoff et al., 2008; Palomero-Gallagher and Zilles, 2017). As well as this it may be noted that the resolution of the PET imaging leaves open the question of whether the relevant receptors are located pre- or post-synaptically (Farrant and Nusser, 2005). This question will be difficult to address using human imaging and so complementary non-human animal-based investigations of the relationship between TV and $GABA_A$ receptors at the timescales studied here is required. Finally, establishing a relationship between TV and rMRGlu/rCBF was done in healthy participants with a high level of ongoing neural activity. It would be interesting to investigate how this relationship changes in states where there is greatly reduced overall neural activity, such as anesthesia or in patients with disorders of consciousness (Huang et al., 2016).

To conclude, using a combination of BOLD fMRI, ASL, FDG-PET, and FMZ-PET in two independent groups of participants, we show that TV in the visual cortex is positively correlated with energy consumption in the same region. The level of TV is reduced with the opening of the eyes while rCBF is increased, suggesting that the constraint of activity over time is an active process that is likely to involve an increase in inhibitory activity. These findings provide insight into the neural processes underlying TV in the human brain, as well as into the mechanisms potentially involved in regulating this when the behavioral state alters.

ACKNOWLEDGMENTS

The authors would like to thank all the participants for their time and effort. Thanks also to the technical and support staff at the Shuang-Ho Hospital and Montreal Neurological Institute for their skillful contribution. The authors are grateful to Dr. Gang Chen (NIMH AFNI) for his support with data analysis. This work was supported by grants to TL from Taiwan's Ministry of Science and Technology (MOST 106-2410-H-038-003-MY3, MOST 105-2410-H-038-004-MY1 and 104-2420-H-038-001-MY3) and Ministry of Health and Welfare (104-TDU-B-212-113001, 105-TDU-B-212-133018). PQ received support from the National Science Foundation of China (31771249). NWD acknowledges support from the National Science Foundation of China (31471072); Taiwan Ministry of Science and Technology (105-2410-H-038-006-MY3, 105-2410-H-038-005-MY2); and from Taipei Medical University (104-6402-006-110). GN acknowledges support from the Canadian Institutes of Health Research (201103MOP-244752-BSB-CECA-179644; 201103CCI-248496-CCI-CECA-179644) and the Michael Smith Foundation (200809EJL-194083-EJL-CECA-179644). The authors declare no conflicts of interest.

REFERENCES

Aiello M, Salvatore E, Cachia A, Pappatà S, Cavaliere C, Prinster A, Nicolai E, Salvatore M, Baron J, Quarantelli M (2015) Relationship between simultaneously acquired resting-state regional cerebral glucose metabolism and functional MRI: A PET/MR hybrid scanner study. NeuroImage. https://doi.org/10.1016/j.neuroimage.2015.03.017.

Arancibia-Cárcamo IL, Kittler JT (2009) Regulation of GABA(A) receptor membrane trafficking and synaptic localization. Pharmacol Ther 123:17–31. https://doi.org/10.1016/j.pharmthera.2009.03.012.

Armbruster-Genc DJN, Ueltzhoffer K, Fiebach CJ (2016) Brain signal variability differentially affects cognitive flexibility and cognitive stability. J Neurosci 36:3978–3987. https://doi.org/10.1523/JNEUROSCI.2517-14.2016.

Barry RJ, Clarke AR, Johnstone SJ, Magee CA, Rushby JA (2007) EEG differences between eyes-closed and eyes-open resting conditions. Clin Neurophysiol 118:2765–2773. https://doi.org/10.1016/j.clinph.2007.07.028.

Behzadi Y, Restom K, Liau J, Liu TT (2007) A component based noise correction method (CompCor) for BOLD and perfusion based fMRI. NeuroImage 37:90–101. https://doi.org/10.1016/j.neuroimage.2007.04.042.

Bianciardi M, Fukunaga M, van Gelderen P, Horovitz SG, de Zwart JA, Duyn JH (2009) Modulation of spontaneous fMRI activity in human visual cortex by behavioral state. NeuroImage 45:160–168. https://doi.org/10.1016/j.neuroimage.2008.10.034.

Cha Y-HK, Jog MA, Kim Y-C, Chakrapani S, Kraman SM, Wang DJJ (2013) Regional correlation between resting state FDG PET and pCASL perfusion MRI. J Cereb Blood Flow Metab 33:1909–1914. https://doi.org/10.1038/jcbfm.2013.147.

Chen Y, Wolk DA, Reddin JS, Korczykowski M, Martinez PM, Musiek ES, Newberg AB, Julin P, Arnold SE, Greenberg JH, Detre JA (2011) Voxel-level comparison of arterial spin-labeled perfusion MRI and FDG-PET in Alzheimer disease. Neurology 77:1977–1985. https://doi.org/10.1212/WNL.0b013e31823a0ef7.

Costes N, Dagher A, Larcher K, Evans AC, Collins DL, Reilhac A (2009) Motion correction of multi-frame PET data in neuroreceptor mapping: simulation based validation. NeuroImage 47:1496–1505. https://doi.org/10.1016/j.neuroimage.2009.05.052.

Deco G, Jirsa V, McIntosh AR, Sporns O, Kötter R (2009) Key role of coupling, delay, and noise in resting brain fluctuations. Proc Natl Acad Sci USA 106:10302–10307. https://doi.org/10.1073/pnas.0901831106.

Deco G, Jirsa VK (2012) Ongoing cortical activity at rest: criticality, multistability, and ghost attractors. J Neurosci 32:3366–3375. https://doi.org/10.1523/JNEUROSCI.2523-11.2012.

Du AT, Jahng GH, Hayasaka S, Kramer JH, Rosen HJ, Gorno-Tempini ML, Rankin KP, Miller BL, Weiner MW, Schuff N (2006) Hypoperfusion in frontotemporal dementia and Alzheimer disease by arterial spin labeling MRI. Neurology 67:1215–1220. https://doi.org/10.1212/01.wnl.0000238163.71349.78.

Duncan NW, Northoff G (2012) Overview of potential procedural and participant-related confounds for neuroimaging of the resting state. J Psychiatry Neurosci 38:84–96.

Duncan NW, Wiebking C, Northoff G (2014) Associations of regional GABA and glutamate with intrinsic and extrinsic neural activity in humans: a review of multimodal imaging studies. Neurosci Biobehav Rev 47:36–52. https://doi.org/10.1016/j.neubiorev.2014.07.016.

Eickhoff SB, Rottschy C, Kujovic M, Palomero-Gallagher N, Zilles K (2008) Organizational principles of human visual cortex revealed by receptor mapping. Cereb Cortex N. Y. N 1991(18):2637–2645. https://doi.org/10.1093/cercor/bhn024.

Farrant M, Nusser Z (2005) Variations on an inhibitory theme: phasic and tonic activation of GABA(A) receptors. Nat Rev Neurosci 6:215–229. https://doi.org/10.1038/nrn1625.

Ferri F, Costantini M, Huang Z, Perrucci MG, Ferretti A, Romani GL, Northoff G (2015) Intertrial variability in the premotor cortex accounts for individual differences in peripersonal space. J Neurosci 35:16328–16339. https://doi.org/10.1523/JNEUROSCI.1696-15.2015.

Fingelkurts AA, Fingelkurts AA, Kivisaari R, Pekkonen E, Ilmoniemi RJ, Kähkönen S (2004) The interplay of lorazepam-induced brain oscillations: microstructural electromagnetic study. Clin Neurophysiol 115:674–690. https://doi.org/10.1016/j.clinph.2003.10.025.

Frey KA, Holthoff VA, Koeppe RA, Jewett DM, Kilbourn MR, Kuhl DE (1991) Parametric in vivo imaging of benzodiazepine receptor distribution in human brain. Ann Neurol 30:663–672.

Galazzo IB, Mattoli MV, Pizzini FB, De Vita E, Barnes A, Duncan JS, Jager R, Golay X, Bomanji JB, Koepp M, Groves AM, Fraioli F (2016) Cerebral metabolism and perfusion in MR-negative individuals with refractory focal epilepsy assessed by simultaneous acquisition of 18F-FDG PET and arterial spin labeling. NeuroImage Clin 11:648–657. https://doi.org/10.1016/j.nicl.2016.04.005.

Galow LV, Schneider J, Lewen A, Ta T-T, Papageorgiou IE, Kann O (2014) Energy substrates that fuel fast neuronal network oscillations. Front Neurosci 8:398. https://doi.org/10.3389/fnins.2014.00398.

Garrett DD, Kovacevic N, McIntosh AR, Grady CL (2012) The modulation of BOLD variability between cognitive states varies by age and processing speed. Cereb Cortex 23:684–693. https://doi.org/10.1093/cercor/bhs055.

Garrett DD, McIntosh AR, Grady CL (2014) Brain signal variability is parametrically modifiable. Cereb Cortex 24:2931–2940. https://doi.org/10.1093/cercor/bht150.

Garrett DD, Samanez-Larkin GR, MacDonald SWS, Lindenberger U, McIntosh AR, Grady CL (2013) Moment-to-moment brain signal variability: a next frontier in human brain mapping? Neurosci Biobehav Rev 37:610–624. https://doi.org/10.1016/j.neubiorev.2013.02.015.

He BJ (2011) Scale-free properties of the functional magnetic resonance imaging signal during rest and task. J Neurosci 31:13786–13795. https://doi.org/10.1523/JNEUROSCI.2111-11.2011.

Hermes M, Hagemann D, Britz P, Lieser S, Rock J, Naumann E, Walter C (2007) Reproducibility of continuous arterial spin labeling perfusion MRI after 7 weeks. Magn Reson Mater Phys Biol Med 20:103–115. https://doi.org/10.1007/s10334-007-0073-3.

Hong I, Chung S, Kim H, Kim Y (2007) Ultra fast symmetry and SIMD-based projection-backprojection (SSP) algorithm for 3-D PET image reconstruction. IEEE Trans Med Imaging 26:789–803. https://doi.org/10.1109/TMI.2002.808360.

Howarth C (2014) The contribution of astrocytes to the regulation of cerebral blood flow. Front Neurosci 8:1–9. https://doi.org/10.3389/fnins.2014.00103.

Huang Z, Zhang J, Wu J, Qin P, Wu X, Wang Z, Dai R, Li Y, Liang W, Mao Y, Yang Z, Zhang J, Wolff A, Northoff G (2016) Decoupled temporal variability and signal synchronization of spontaneous brain activity in loss of consciousness: an fMRI study in anesthesia. NeuroImage 124:693–703. https://doi.org/10.1016/j.neuroimage.2015.08.062.

Hudson HM, Larkin RS (1994) Accelerated image reconstruction using ordered subsets of projection data. IEEE Trans Med Imaging 13:601–609. https://doi.org/10.1109/42.363108.

Hyder F, Fulbright RK, Shulman RG, Rothman DL (2013) Glutamatergic function in the resting awake human brain is supported by uniformly high oxidative energy. J Cereb Blood Flow Metab 33:339–347. https://doi.org/10.1038/jcbfm.2012.207.

Hyder F, Rothman DL (2011) Evidence for the importance of measuring total brain activity in neuroimaging. Proc Natl Acad Sci USA 108:5475–5476. https://doi.org/10.1073/pnas.1102026108.

Jacob TC, Moss SJ, Jurd R (2008) GABA(A) receptor trafficking and its role in the dynamic modulation of neuronal inhibition. Nat Rev Neurosci 9:331–343. https://doi.org/10.1038/nrn2370.

Jacobson-Pick S, Richter-Levin G (2012) Short- and long-term effects of juvenile stressor exposure on the expression of GABAA receptor subunits in rats. Stress 15:416–424. https://doi.org/10.3109/10253890.2011.634036.

Jaffer S, Vorobyov V, Kind PC, Sengpiel F (2012) Experience-dependent regulation of functional maps and synaptic protein expression in the cat visual cortex. Eur J Neurosci 35:1281–1294. https://doi.org/10.1111/j.1460-9568.2012.08044.x.

Jao T, Vértes PE, Alexander-Bloch AF, Tang I-N, Yu Y-C, Chen J-H, Bullmore ET (2012) Volitional eyes opening perturbs brain dynamics and functional connectivity regardless of light input. NeuroImage 69:21–34. https://doi.org/10.1016/j.neuroimage.2012.12.007.

Jirmann K-U, Pernberg J, Eysel UT (2009) Region-specificity of GABAA receptor mediated effects on orientation and direction selectivity in cat visual cortical area 18. Exp Brain Res 192:369. https://doi.org/10.1007/S00221-008-1583-6.

Jueptner M, Weiller C (1995) Review: does measurement of regional cerebral blood flow reflect synaptic activity? Implications for PET and fMRI. NeuroImage. https://doi.org/S1053811985710178 [pii].

Kann O, Papageorgiou IE, Draguhn A (2014) Highly energized inhibitory interneurons are a central element for information processing in cortical networks. J Cereb Blood Flow Metab Off J Int Soc Cereb Blood Flow Metab 34:1270–1282. https://doi.org/10.1038/jcbfm.2014.104.

Katzner S, Busse L, Carandini M (2011) GABAA inhibition controls response gain in visual cortex. J Neurosci 31:5931–5941. https://doi.org/10.1523/JNEUROSCI.5753-10.2011.

la Fougère C, Grant S, Kostikov A, Schirrmacher R, Gravel P, Schipper HM, Reader A, Evans A, Thiel A (2011) Where in-vivo imaging meets cytoarchitectonics: the relationship between cortical thickness and neuronal density measured with high-resolution [18F]flumazenil-PET. NeuroImage 56:951–960. https://doi.org/10.1016/j.neuroimage.2010.11.015.

Li Z, Zhu Y, Childress AR, Detre JA, Wang Z (2012) Relations between BOLD fMRI-derived resting brain activity and cerebral blood flow. PLoS ONE 7:e44556. https://doi.org/10.1371/journal.pone.0044556.

Liang X, Zou Q, He Y, Yang Y (2013) Coupling of functional connectivity and regional cerebral blood flow reveals a physiological basis for network hubs of the human brain. Proc Natl Acad Sci USA 110:1929–1934. https://doi.org/10.1073/pnas.1214900110.

Liefaard LC, Ploeger BA, Molthoff CFM, de Jong HWAM, Dijkstra J, van der Weerd L, Lammertsma AA, Danhof M, Voskuyl RA (2009) Changes in GABAA receptor properties in amygdala kindled animals: in vivo studies using [11C]flumazenil and positron

emission tomography. Epilepsia 50:88–98. https://doi.org/10.1111/j.1528-1167.2008.01763.x.

Logan J, Fowler JSJS, Volkow ND, Wang GJG, Ding YYS, Alexoff DLDL, Volkow D (1996) Distribution volume ratios without blood sampling from graphical analysis of PET data. J Cereb Blood Flow Metab 16:834–840.

Logothetis NK (2008) What we can do and what we cannot do with fMRI. Nature 453:869–878. https://doi.org/10.1038/nature06976.

Martino M, Magioncalda P, Huang Z, Conio B, Piaggio N, Duncan NW, Rocchi G, Escelsior A, Marozzi V, Wolff A, Inglese M, Amore M, Northoff G (2016) Contrasting variability patterns in the default mode and sensorimotor networks balance in bipolar depression and mania. Proc Natl Acad Sci 113:4824–4829. https://doi.org/10.1073/pnas.1517558113.

Mennes M, Zuo X-N, Kelly C, Di Martino A, Zang Y-F, Biswal B, Castellanos FX, Milham MP (2011) Linking inter-individual differences in neural activation and behavior to intrinsic brain dynamics. NeuroImage 54:2950–2959. https://doi.org/10.1016/j.neuroimage.2010.10.046.

Newberg AB, Wang J, Rao H, Swanson RL, Wintering N, Karp JS, Alavi A, Greenberg JH, Detre JA (2005) Concurrent rCBF and CMRGlc changes during human brain activation by combined fMRI-PET scanning. NeuroImage 28:500–506. https://doi.org/10.1016/j.neuroimage.2005.06.040.

Nugent AC, Martinez A, D'Alfonso A, Zarate CA, Theodore WH (2015) The relationship between glucose metabolism, resting-state fMRI BOLD signal, and GABAA-binding potential: a preliminary study in healthy subjects and those with temporal lobe epilepsy. J Cereb Blood Flow Metab 35:583–591. https://doi.org/10.1038/jcbfm.2014.228.

Ogawa S, Lee TM, Kay AR, Tank DW (1990) Brain magnetic resonance imaging with contrast dependent on blood oxygenation. Proc Natl Acad Sci USA 87:9868–9872.

Palomero-Gallagher N, Zilles K (2017) Cortical layers: Cyto-, myelo-, receptor- and synaptic architecture in human cortical areas. NeuroImage. https://doi.org/10.1016/j.neuroimage.2017.08.035.

Prevett MC, Lammertsma AA, Brooks DJ, Bartenstein PA, Patsalos PN, Fish DR, Duncan JS (1995) Benzodiazepine-GABAA receptors in idiopathic generalized epilepsy measured with [11C]flumazenil and positron emission tomography. Epilepsia 36:113–121.

Qin P, Duncan NW, Wiebking C, Gravel P, Lyttelton O, Hayes DJ, Verhaeghe J, Kostikov A, Schirrmacher R, Reader AJ, Northoff G (2012) GABAA receptors in visual and auditory cortex and neural activity changes during basic visual stimulation. Front Hum Neurosci 6:1–13. https://doi.org/10.3389/fnhum.2012.00337.

Riedl V, Bienkowska K, Strobel C, Tahmasian M, Grimmer T, Forster S, Friston KJ, Sorg C, Drzezga A, Förster S (2014) Local activity determines functional connectivity in the resting human brain: a simultaneous FDG-PET/fMRI Study. J Neurosci 34:6260–6266. https://doi.org/10.1523/JNEUROSCI.0492-14.2014.

Sabolek HR, Swiercz WB, Lillis KP, Cash SS, Huberfeld G, Zhao G, Ste Marie L, Clemenceau S, Barsh G, Miles R, Staley KJ (2012) A candidate mechanism underlying the variance of interictal spike propagation. J Neurosci 32:3009–3021. https://doi.org/10.1523/JNEUROSCI.5853-11.2012.

Salmi E, Aalto S, Hirvonen J, Långsjö JW, Maksimow AT, Oikonen V, Metsähonkala L, Virkkala J, Någren K, Scheinin H (2008) Measurement of GABAA receptor binding in vivo with [11C] flumazenil: a test-retest study in healthy subjects. NeuroImage 41:260–269. https://doi.org/10.1016/j.neuroimage.2008.02.035.

Samanez-Larkin GR, Kuhnen CM, Yoo DJ, Knutson B (2010) Variability in nucleus accumbens activity mediates age-related suboptimal financial risk taking. J Neurosci 30:1426–1434. https://doi.org/10.1523/JNEUROSCI.4902-09.2010.

Shew WL, Yang H, Yu S, Roy R, Plenz D (2011) Information capacity and transmission are maximized in balanced cortical networks with neuronal avalanches. J Neurosci 31:55–63. https://doi.org/10.1523/JNEUROSCI.4637-10.2011.

Takahashi T (2013) Complexity of spontaneous brain activity in mental disorders. Prog Neuropsychopharmacol Biol Psychiatry 45:258–266. https://doi.org/10.1016/j.pnpbp.2012.05.001.

van Vreeswijk C, Sompolinsky H (1996) Chaos in neuronal networks with balanced excitatory and inhibitory activity. Science 274:1724–1726.

Wong CW, DeYoung PN, Liu TT (2016) Differences in the resting-state fMRI global signal amplitude between the eyes open and eyes closed states are related to changes in EEG vigilance. NeuroImage 124:24–31. https://doi.org/10.1016/j.neuroimage.2015.08.053.

Wutte MG, Smith MT, Flanagin VL, Wolbers T (2011) Physiological signal variability in hMT+ reflects performance on a direction discrimination task. Front Psychol 2:185. https://doi.org/10.3389/fpsyg.2011.00185.

Xiao Y, Huang X, Van Wert S, Barreto E, Wu J, Gluckman BJ, Schiff SJ (2012) The role of inhibition in oscillatory wave dynamics in the cortex. Eur J Neurosci 36:2201–2212.

Yeo B, Krienen F (2011) The organization of the human cerebral cortex estimated by intrinsic functional connectivity. J Neurophysiol 106:1125–1165. https://doi.org/10.1152/jn.00338.2011.

Zou Q, Yuan B, Gu H, Liu D, Wang DJJ, Gao J-H, Yang Y, Zang Y-F (2015) Detecting static and dynamic differences between eyes-closed and eyes-open resting states using ASL and BOLD fMRI. PLoS ONE 10:e0121757. https://doi.org/10.1371/journal.pone.0121757.

(Received 17 January 2018, Accepted 22 February 2018)
(Available online 10 March 2018)